Journal of Computational Physics **174,** 1–11 (2001)
doi:10.1006/jcph.2001.6867, available online at http://www.idealibrary.com on IDEAL®

Fast Computations of Wave Propagation in an Inhomogeneous Plasma by a Pulse Compression Method

S. Hacquin,* S. Heuraux,* M. Colin,* and G. Leclert†

*Laboratoire de Physique des Milieux Ionisés, Unité CNRS 7040, Université Henri Poincaré-Nancy I, BP 239, F54 506 Vandœuvre-lès-Nancy Cedex, France; and †Laboratoire PIIM (Turbulence Plasma), Unité 6633 CNRS-Université de Provence, Centre de St-Jêrome, Case 321, F13 397 Marseille Cedex 20, France

Received August 24, 2000; revised June 15, 2001

A pulse compression method is proposed to simulate the propagation of a pulse in an inhomogeneous plasma. It allows very fast computations compared to the usual time-dependent code. The characteristics as well as the limitations of this method are discussed. In particular the phase shift of the pulse frequency components is analyzed for different kinds of density profiles. The validity of using this method under typical conditions in fusion plasmas is then discussed. © 2001 Elsevier Science

1. INTRODUCTION

The propagation of electromagnetic waves in inhomogeneous plasmas is an active field of research, in particular for diagnostics in thermonuclear fusion and ionosphere plasmas [1]. The cold plasma approximation is usually used to describe wave propagation in such media [2]. Under this cold plasma approximation and assuming stationary and inhomogeneous density, the one-dimensional (1D) propagation of a wave is then governed by the following time-dependent equation

$$\left[\partial_{tt}^2 - c^2\partial_{xx}^2 + \omega_{pe}^2(x)\right] E(x,t) = 0. \tag{1}$$

This equation is valid in unmagnetized plasmas as well as for the ordinary mode polarization in magnetized plasmas. Analytical solutions can be obtained in the case of a homogeneous plasma [3]. For the extraordinary mode one must solve a more complex set of equations [4]. To simulate the propagation of a pulse in an inhomogeneous plasma, Eq. (1) has to be solved numerically [5]. Owing to the dependence on both variables x and t, time-dependent codes solving Eq. (1) require a long computation time. We propose here an alternative method inspired by techniques used in electronic, photonic, and radar applications called

0021-9991/01 $35.00

the pulse compression method. This method is based on the decomposition of a pulse in the relevant set of monochromatic waves at different frequencies. Thus, a Fourier analysis of the phases (and the amplitudes in the presence of multidimensional effects) of these successive waves contained in a long wave train gives the same information as the equivalent pulse. The terminology of pulse compression is derived from the fact that the equivalent pulse is usually much shorter than the wave train with its successive frequencies. This aspect allows in particular improvement in the signal-to-noise ratio and thus in measurement precision. More details about the technical aspects of the method can be found, for example, in Ref. [6]. The pulse compression method has already been proposed for density measurement experiments in fusion plasmas [7]. For simplicity, only the case of the ordinary mode polarization is presented in this paper but the proposed method can be similarly applied to the extraordinary mode. The principle of the pulse compression method is presented in Section 2. Section 3 is devoted to the evaluation of the phase needed to apply this method. Its validity and its speed are discussed in Section 4 based on comparisons with a time-dependent code.

2. PRINCIPLE OF THE PULSE COMPRESSION METHOD

The pulse compression method relies on the fact that a pulse can be decomposed in a set of discrete frequencies. Consider for simplicity a wave with a Gaussian envelop at $t = t_i$,

$$E_i(x) = E_0\, e^{i(k_0 x)} e^{-4(x/\sigma)^2}, \tag{2}$$

where k_0 is the wavenumber in vacuum and σ is the width at half amplitude (defined as amplitude e^{-1}). The corresponding spectrum of this signal has also a Gaussian shape:

$$S(k) = \int_{-\infty}^{+\infty} E_i(x) e^{-ikx}\, dx = E_0 \frac{\sqrt{\pi}}{2} \sigma e^{-\left[\frac{\sigma}{4}(k-k_0)\right]^2}. \tag{3}$$

Each component of this spectrum is phase shifted after the pulse propagation in the plasma. If the phase $\phi(k)$ is known or computed for all components, an inverse fast Fourier transform (FFT) permits obtainment of the pulse after propagation in the plasma at $t = t_f$ [8]:

$$E_f(x) = \frac{1}{2\pi} \int_{-\infty}^{+\infty} S(k) e^{-i\phi(k)} e^{ikx}\, dk. \tag{4}$$

In the following the amplitude of the pulse after propagation will be normalized to the initial amplitude E_0. This method implies that the phase shift for each frequency of the pulse is independent of time. It is valid as long as the temporal history of the signal propagation is not affected by nonlinear temporal effects. The different models which can be used to calculate the phase are presented in the next section.

To apply a numerical procedure, Eq. (4) has to be sampled:

$$E_f(x) = \frac{1}{2\pi} \sum_{i=1}^{n} S(k_i) e^{-i\phi(k_i)} e^{ik_i x} \delta k. \tag{5}$$

The parameter δk is important for calculating the final pulse with sufficient accuracy. First, δk has to be small enough to allow a good definition of the k-spectrum of the initial pulse.

At least 20 components are typically needed to define the k-spectrum for a realistic pulse used in fusion plasmas. The parameter δk also imposes the length L of the spatial domain in which the final signal is obtained:

$$L = \frac{2\pi}{\delta k}. \tag{6}$$

It is thus important to be sure that this length is larger than the equivalent path of the pulse in vacuum. In our procedure, we have chosen the center of the spatial domain as the origin so that this domain takes place from $-L/2$ up to $+L/2$. As the initial pulse is centered at $x = 0$, the equivalent path of the pulse in vacuum must be smaller than $L/2$ to avoid any ambiguity. The equivalent path in vacuum covered by the pulse is then directly deduced from the position of the reconstructed signal.

Another characteristic of this method is the number of points n used for the FFT. First, a standard zero padding technique is made to fix this number as a power of 2. And this number must be high enough to have sufficient accuracy in real space. Indeed, the space step δx is given by

$$\delta x = \frac{2\pi}{n\delta k}. \tag{7}$$

In order to obtain good accuracy in the reconstructed signal, δx has to be small compared to the typical wavelength of this signal. In addition to needing a small δk, this condition requires a sufficient number of points n.

Consider for example an initial Gaussian pulse with a frequency $f = 60$ GHz (or a wavenumber $k_0 = 12.5$ rad cm^{-1}) and a spectral width $\Delta f = 4$ GHz at amplitude e^{-1} (which is equivalent to a spatial width of about 9.5 cm or a duration of the order of 0.31 ns). Now we want to study by the pulse compression method the propagation of this pulse in plasma. Two parameters have then to be defined: the wavenumber step δk and the number of points n used for the FFT. To avoid truncating effects, we define the Gaussian pulse spectrum up to an amplitude e^{-4}. The width at amplitude e^{-4} is twice the one at e^{-1}. If we choose 100 points to define the spectrum, the wavenumber step is then given by

$$\delta k = \frac{2\pi}{c}\,\delta f = 1.67\,\text{rad m}^{-1}, \tag{8}$$

with $\delta f = 2\Delta f/100 = 80$ MHz. The equivalent path in vacuum of the pulse has to be smaller than $\pi/\delta k$, equal to about 2 m in this case (which is equivalent to a propagation time of 6.6 ns). The number of points n for the FFT has then to be defined which fixes the precision of the reconstructed signal. If we impose 100 points per wavelength (that is large enough to have a good definition), the number n can be deduced from Eq. (7):

$$n = \frac{2\pi}{\delta k}\frac{1}{\delta x} = \frac{2\pi}{\delta k}\frac{100}{\lambda} = 75{,}000. \tag{9}$$

Finally n is chosen as the first power of 2 higher than 75,000, which gives $n = 2^{17} = 131{,}072$. If we take $n = 2^{16} = 65{,}536$, the precision will be $\delta x = 5.7\ 10^{-5}$ m, which corresponds to about 87 points per wavelength.

3. MODELS FOR THE EVALUATION OF THE PHASE

The use of the pulse compression method requires evaluation of the phase shift for all components of the pulse spectrum. In order to reduce the time of computation, it is important to optimize the determination of the phase. We show in this section that different models can be used depending on the characteristics of the medium. These models depend on the characteristics of the density profile. For monotonic and smooth profiles, the WKB approximation allows an analytic expression of the phase. In the presence of density fluctuations with small amplitudes, it is also possible to obtain an analytic expression using the Born approximation. If the amplitude of the density fluctuations becomes strong, the phase evaluation requires solving the Helmholtz equation.

3.1. WKB Approximation

In a homogeneous medium, the phase shift of a wave after a length path L is given by

$$\phi(f) = \frac{2\pi}{c} f N L, \tag{10}$$

where c is the velocity of the light in vacuum, f the frequency of the wave, and N the refractive index depending on the medium crossed. In the case of an inhomogeneous plasma, the evaluation of the phase shift is more complicated and requires solving Eq. (1). However, in some cases, we can assume that the medium properties vary so slowly that it is possible to define locally the wavenumber and the refractive index. This is the WKB approximation, and the phase can be written as

$$\phi(f) = \frac{2\pi}{c} f \int_0^L N(x)\, dx. \tag{11}$$

It requires that the amplitude of the electric field varies very slowly compared to its phase. It is often satisfied for a smooth density profile, except when the wave crosses a cutoff layer or a resonance [2]. For some applications, like reflectometry, which is a diagnostic for density profile measurements in fusion plasmas [9], the wave is reflected by a cutoff layer. In this case, the WKB approximation is no longer valid in the cutoff-layer region. However if we assume a linear density profile in this region, it is possible to express the electric field from the Airy functions [10] and the phase shift can be written [11] as

$$\phi(f) = \frac{4\pi}{c} f \int_{x_0}^{x_c(f)} N(x)\, dx - \frac{\pi}{2}, \tag{12}$$

where x_0 and $x_c(f)$ are, respectively, the plasma-edge and cutoff-layer positions. In Eq. (12) the factor 2 introduced in the integral term is due to the return path of the wave. Moreover, the term $-\pi/2$ is induced by the reflection on the cutoff layer.

Let us consider an initial pulse with a Gaussian shape, a frequency $f = 60$ GHz, and a spectrum width at half amplitude $\Delta f = 5$ GHz corresponding to a spatial width

$$L_i = \frac{4c}{\pi \Delta f} = 7.6\,\text{cm}. \tag{13}$$

In the following, we simulate the propagation of this pulse in homogeneous and unmagnetized plasma characterized by a plasma frequency $f_p = 40$ GHz. Assuming a path

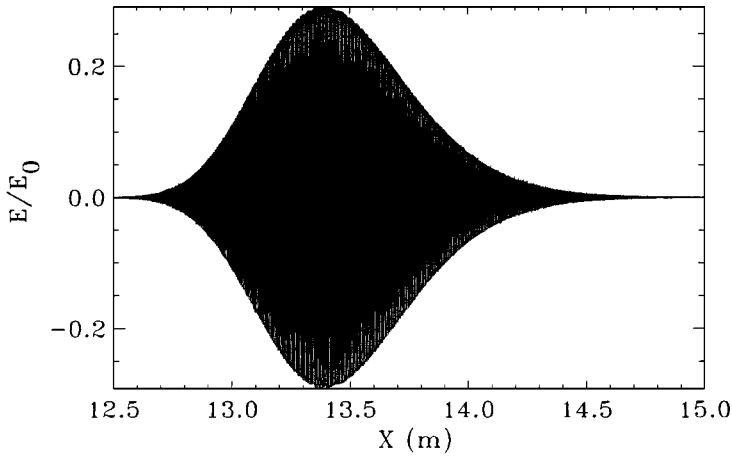

FIG. 1. Signal after propagation in a homogeneous plasma computed by the pulse compression method using the WKB approximation.

length $L = 10$ m the phase shift for each component of the spectrum is evaluated according to Eq. (11). The final signal computed after FFT is represented in Fig. 1. The position of this signal $x = 13.4$ m agrees with the theoretical result and corresponds to the path the pulse would have covered in vacuum (which is equal to the time of propagation multiplied by c). We can also notice a significant broadening of the pulse as well as an asymmetry in its shape. This is induced by dispersive effects occurring in dielectric media [12] as well as in plasmas [13]. The WKB approximation is then well adapted for study of these dispersive effects in plasmas with monotonic and smooth density profiles.

3.2. Born Approximation

In typical fusion or ionosphere plasmas, the density profile presents significant fluctuations so that the WKB approximation fails. In the case of small-amplitude density fluctuations, only the first-order term of the perturbation series can be kept. This hypothesis, called the Born approximation, allows an analytical evaluation of the phase shift for different types of fluctuations [11, 14].

An example is considered for a linear density profile ($n_0 = 6 \times 10^{19}\,\mathrm{m}^{-3}$, $R = 0.5\,\mathrm{m}$) and a density fluctuation with a Gaussian shape, a wavenumber $k_f = 1.5\ \mathrm{cm}^{-1}$, an amplitude $a_f = \delta n_0/n_c = 0.01$, and a width at half amplitude $d_f = 10$ cm. The initial pulse with a frequency $f = 50$ GHz and a width equal to 50 cm is reflected by a cutoff layer at $x_c = 26.25$ cm. According to the Born approximation, the phase variation induced by the fluctuations is given by [11]

$$\Delta\phi = -\sqrt{\pi}k_0\left(\frac{L}{k_f}\right)^{1/2}\frac{\delta n_0}{n_c}\cos[k_f(x_c - x_f) + \pi/4]\exp\left[-\frac{(x_c - x_f)^2}{D_f^2}\right], \qquad (14)$$

where k_0, δn_0, x_c, and n_c are, respectively, the wavenumber in vacuum, the amplitude of the fluctuation, the cutoff-layer position, and the critical density. For a linear density profile, the gradient length L is equal to the distance from the plasma edge up to the cutoff layer.

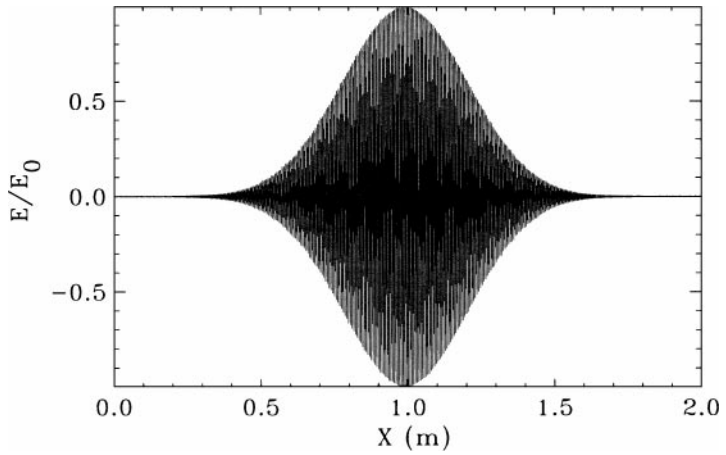

FIG. 2. Reflected pulse in the presence of density fluctuations with small amplitude computed by the pulse compression method using the Born approximation.

The total phase is then obtained from

$$\phi^* = \phi + \Delta\phi, \tag{15}$$

where ϕ is the phase given by the WKB theory for a density profile without fluctuation. The pulse reflected by the plasma for the fluctuation position $x_f = 26.25$ cm and computed by the pulse compression method using Eqs. (14) and (15) is shown in Fig. 2. It is clear that there is no significant deformation in the signal shape. In fact, the dominant physical process is the oscillation of the cutoff layer. Consequently, a variation in the time of flight (time between the initial and reflected pulses) should be noticed. As the time of flight is equal to the derivative of the phase with regard to the pulsation, this variation is obtained by deriving Eq. (15):

$$\tau^*(\omega) = \frac{\partial\phi^*}{\partial\omega} = \frac{\partial\phi}{\partial\omega} + \frac{\partial\Delta\phi}{\partial\omega} = \tau(\omega) + \Delta\tau(\omega). \tag{16}$$

Let us notice that the time-of-flight variations are expressed as a function of the pulsation ω but it is equivalent to expressing them as a function of the fluctuation position. We have thus determined the variations of the time of flight as a function of the density fluctuation position from the reflected signals computed by the pulse compression method. The results compared to the term $\Delta\tau$ of Eq. (16) are presented in Fig. 3. The very small discrepancies between the analytical curve and the computed one are induced by the numerical method used to evaluate the time of flight. The good agreement shows the validity of the pulse compression method using Born approximation in the case of density fluctuations with small wavenumber. A limit of validity for the Born approximation is given in Ref. [15].

3.3. Helmholtz Equation

In the case of density fluctuations with a large amplitude, the Born approximation is no longer valid. In that case, a computation of Eq. (1) is needed to evaluate the phase.

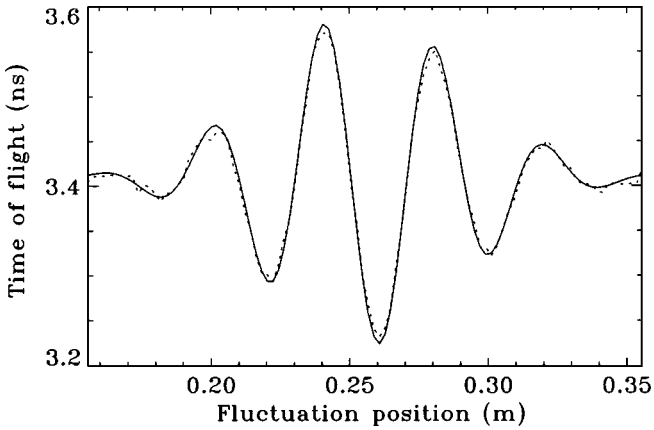

FIG. 3. Time-of-flight variations as a function of the density fluctuation position: comparison between the theoretical expression of the Born approximation (full line) and the variations deduced from the pulses computed by the pulse compression method (dotted line).

However monochromatic waves can be considered for each frequency component of the pulse spectrum. The time-dependent Eq. (1) can then be reduced to the following Helmholtz equation:

$$\left[\frac{d^2}{dx^2} + k_0^2\, N^2(x)\right] E(x) = 0. \tag{17}$$

A numerical code solving this equation has been developed [16]. The pulse compression method can then be used from the phases computed by the Helmholtz code.

An example is shown for a linear density profile ($n_0 = 6 \times 10^{19}$ m^{-3}, $R = 0.5$ m) and a density fluctuation with a wavenumber $k_f = 18\,\mathrm{cm}^{-1}$, an amplitude $a_f = \delta n_0/n_c = 0.03$, and a width at half amplitude $d_f = 8$ cm. This fluctuation is located at $x = 18$ cm, where the Bragg backscattering condition is satisfied [17]. In such cases, one part of the wave is backscattered by the fluctuations. The reconstructed signal is thus composed from a backscattered pulse and a reflected pulse. The successive pulses with decreasing amplitudes are due to the multiple reflections of the wave between the fluctuations and the cutoff layer, as shown in Fig. 4. From the positions of these different pulses, we can deduce the amplitude and the time of flight for the first backscattered and the reflected pulses ($a_{diff} = 0.37$, $a_{ref} = 0.85$, $\tau_{diff} = 1.4$ ns, $\tau_{ref} = 4.9$ ns). The values of time of flight are similar to those obtained theoretically in the case of a linear density profile.

4. DOMAINS OF VALIDITY OF THE PULSE COMPRESSION METHOD

The pulse compression method presented in this paper is efficient as long as Eqs. (4) and (5) are valid. It amounts to saying that no nonlinear temporal effects play a role in the interaction between the wave and the plasma (in the opposite case, coupling between different Fourier components would distort the signal). We propose in this section to verify the validity of the pulse compression method by comparisons with the time-dependent code. The improvements in times of computation are also shown and discussed.

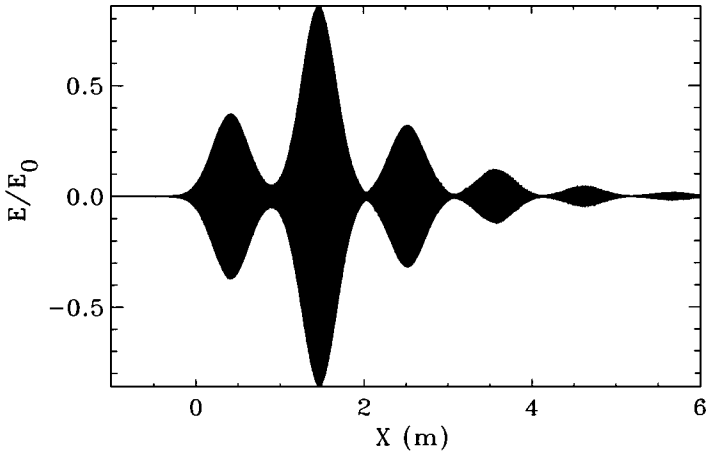

FIG. 4. Reflected pulse computed by the pulse compression method using the Helmholtz equation: the case of a Bragg-resonant density fluctuation.

4.1. Study of the Validity in the Presence of Realistic Density Fluctuations

In order to validate the pulse compression method, we present here a simulation obtained from the time-dependent code in the same conditions as those presented in Fig. 4. The backward computed signal is shown in Fig. 5. We can see the good agreement with the reflected signal given by the pulse compression method. Let us just notice that a change on the horizontal axis origin has been needed in Fig. 5. Indeed, the horizontal axis represents the real space for the time-dependent code while it corresponds to the equivalent path in vacuum for the pulse compression method.

Various comparative tests have shown that the pulse compression method gives results identical to the time-dependent code (in the limit of the numerical scheme accuracy) as long as no cavity is present in the plasma. Indeed the presence of cavities induces the temporal phenomena of wave trapping which can lead to a discrepancy between the two

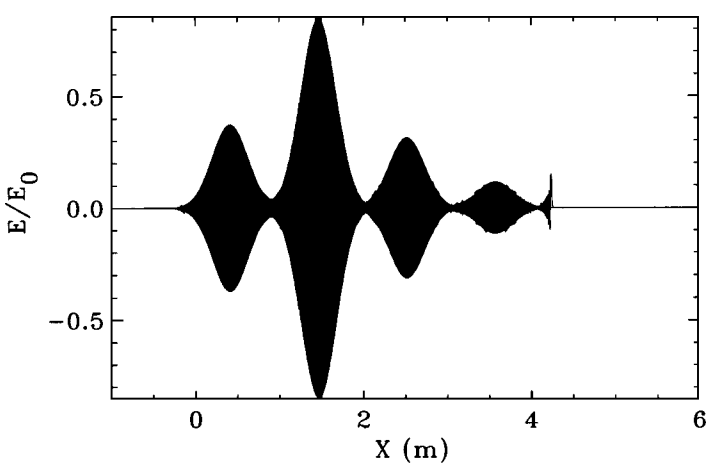

FIG. 5. Reflected pulse computed by the time-dependent code in the same case as presented in Fig. 4 (plasma edge at $x = 3.87$ m).

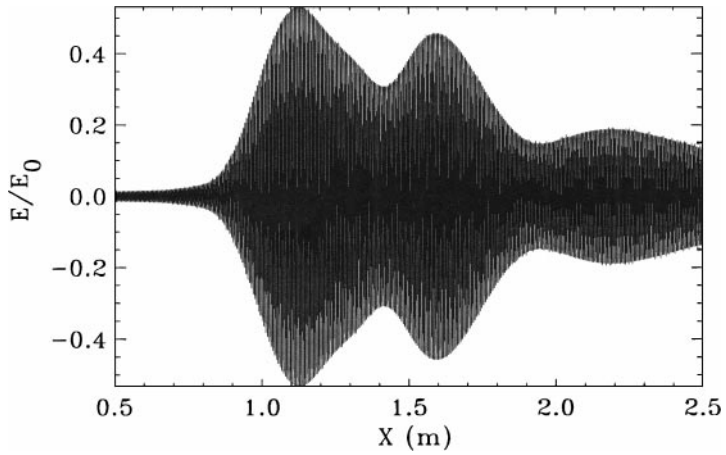

FIG. 6. Reflected pulse computed by the pulse compression method using the Helmholtz equation: the case of hole density in the vicinity of the cutoff layer.

methods (as discussed in the next section). In fusion plasmas for instance, some cavities could be induced by MHD-like as well as microturbulent density fluctuations. However, the typical level of fluctuation in such media is rarely high enough to lead to this scenario.

4.2. Nonlinear Effects: Large Gaussian Density Hole

We consider now the case of a plasma with a density hole of amplitude $a_f = 50\%$ located just behind the cutoff layer at $x_f = 32$ cm. The reflected signals computed by the pulse compression method and the time-dependent code are shown, respectively, in Figs. 6 and 7. In this case we can notice significant differences in the shape of the reflected signal. This is induced by the presence of a subcritical cavity in the evanescent region of the wave. One part of the wave is trapped in the density hole, as shown in Fig. 7 (as the plasma region

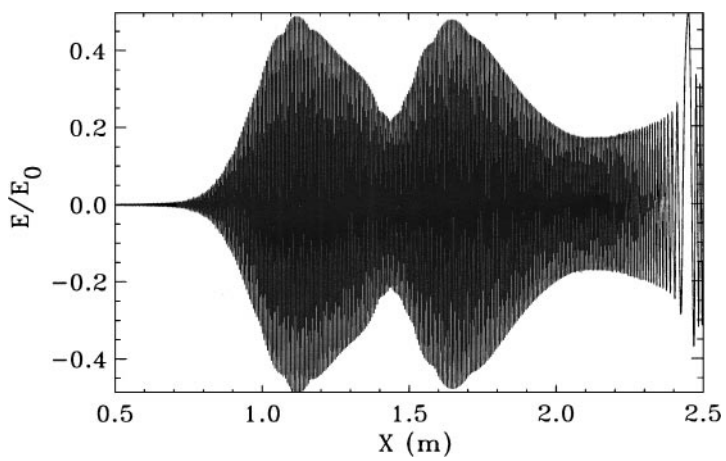

FIG. 7. Reflected pulse computed by the time-dependent code in the same case as presented in Fig. 6 (plasma edge at $x = 2.18$ m).

corresponds to $x > 2.18$ m, the trapping occurs in the vicinity of the cutoff layer located at $x \simeq 2.4$ m). This process of wave trapping depends on the time and frequency components, so the pulse compression method fails. Indeed, the Helmholtz code does not take into account the temporal aspect of the wave–plasma interaction in this case. Consequently, in the presence of such temporal processes as wave trapping, the pulse compression method will be no longer valid.

The dynamical phenomena of wave trapping depend on various parameters, namely the shape of the density profile and, in particular, of the cavity (amplitude, width, ...), as well as on the wave frequency. The process of wave trapping is the strongest when the pulse duration is on the same order of magnitude as the transit time in the cavity. In the case of a Gaussian cavity (as presented in Figs. 6 and 7) we have noticed that the discrepancies (evaluated from the differences in the signal amplitude) between pulse compression and time-dependent methods do not exceed 1% until a density fluctuation amplitude of 20%. The pulse compression method can then be used for various applications, implying fusion plasmas.

4.3. Improvements in Computation Time

To emphasize the speed of the pulse compression method, we compare here the computation time with the time-dependent code. This is exemplified for a pulse propagating in a linear density profile. The incident frequency of this pulse is equal to 60 GHz and the maximal plasma frequency is equal to 65 GHz. The pulse is then reflected by the plasma at the position $x = R(60/65)^2$ where R is the plasma radius. The computations are carried out using various plasma radii. The comparison between the pulse compression method and the time-dependent code is presented in Fig. 8 (a precision of 100 points per wavelength has been chosen for both methods). We can notice that the larger the plasma radius, the higher the improvement in computation time. For a plasma radius $R = 0.25$ m, the pulse compression method is about seven times faster than the time-dependent code while it is at least 50 times faster for $R = 3$ m.

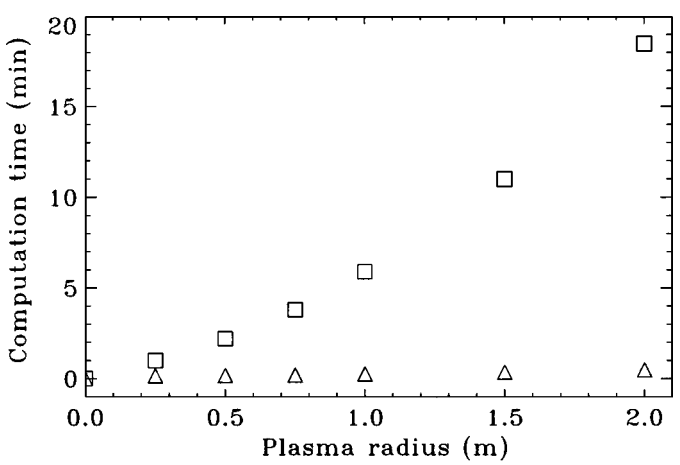

FIG. 8. Comparison of the computation time between the time-dependent code (square symbols) and the pulse compression method (triangle symbols).

5. DISCUSSION

The propagation of electromagnetic waves in plasmas presents numerous applications in the fields of thermonuclear fusion and ionosphere physics. The propagation of a wave in plasmas can rarely be solved analytically and numerical simulations are usually required. Under the cold plasma approximation, we have proposed here a fast method for computing the propagation of a pulse. The major interest of the pulse compression method is that it is incomparably faster than a code solving the time-dependent wave equation. Although this method can be no longer valid in severe conditions, such as those encountered in the presence of strong, localized perturbations (density holes), it is shown that it could be used in typical fusion or ionosphere plasmas. It is for example well adapted for the study of microwave diagnostics in fusion plasmas.

The pulse compression method is valid for different modes of wave propagation as long as the phase evaluation is correct. In the case of a magnetized plasma for example, it can be applied to the ordinary mode polarization as well as to the extraordinary mode polarization. Let us just notice that it is particularly interesting for the extraordinary mode owing to the complex equations solved by a time-dependent code [18]. The main restriction of the pulse compression method is that it requires that the density profile be stationary on a time scale much larger than the incident wave period. To study time-dependent phenomena, more complicated methods based on the resolution of the full set of Maxwell equations are needed.

REFERENCES

1. J. H. Hartfuss, *Plasma Phys. Control. Fusion* **40**, A231 (1998).
2. V. L. Ginzburg, *The Propagation of Electromagnetic Waves in Plasmas* (Gordon and Breach, NY, 1964).
3. B. Nodland and C. J. McKinstrie, *Phys. Rev. E* **56**, 7174 (1997).
4. E. Mazzucato, *Rev. Sci. Instrum.* **69**, 2201 (1998).
5. B. I. Cohen, B. B. Afeyan, A. E. Chou, and N. C. Luhmann Jr., *Plasma Phys. Control. Fusion* **37**, 329 (1995).
6. D. R. Wehner, *High-Resolution Radar*, 2nd ed. (Artech House, Boston, 1995).
7. C. Laviron, P. Millot, and R. Prentice, *Plasma Phys. Control. Fusion* **37**, 975 (1995).
8. S. H. Heijnen, Ph.D. Thesis (University of Utrecht, 1995).
9. A. E. Costley and Members of the ITER Joint Central Team and Home Teams, *Rev. Sci. Instrum.* **70**, 2391 (1999).
10. M. Abramowitz and I. A. Stegun, *Handbook of Mathematical Functions* (Dover, NY, 1965).
11. C. Fanack, I. Boucher, F. Clairet, S. Heuraux, G. Leclert, and X. L. Zou, *Plasma Phys. Control. Fusion* **38**, 1915 (1996).
12. K. E. Oughstun and C. M. Balictsis, *Phys. Rev. Lett.* **77** (11), 2210 (1996).
13. S. Hacquin, S. Heuraux, M. Colin, and G. Leclert, *Plasma Phys. Control. Fusion* **42**, 347 (2000).
14. N. Bretz, *Phys. Fluids* **B4**, 2414 (1992).
15. B. B. Afeyan, A. E. Chou, and B. I. Cohen, *Plasma Phys. Control. Fusion* **37**, 315 (1995).
16. C. Fanack, Ph.D. Thesis (University of Nancy, 1997).
17. X. L. Zou, L. Laurent, and J. M. Rax, *Plasma Phys.* **33**, 903 (1991).
18. B. I. Cohen, L. L. LoDestro, E. B. Hooper, and T. A. Casper, *Plasma Phys. Control. Fusion* **40**, 75 (1998).